LETTER

doi:10.1038/nature14514

Activating positive memory engrams suppresses depression-like behaviour

Steve Ramirez[1], Xu Liu‡, Christopher J. MacDonald[1], Anthony Moffa[1], Joanne Zhou[1], Roger L. Redondo[1,2] & Susumu Tonegawa[1,2]

Stress is considered a potent environmental risk factor for many behavioural abnormalities, including anxiety and mood disorders[1,2]. Animal models can exhibit limited but quantifiable behavioural impairments resulting from chronic stress, including deficits in motivation, abnormal responses to behavioural challenges, and anhedonia[3–5]. The hippocampus is thought to negatively regulate the stress response and to mediate various cognitive and mnemonic aspects of stress-induced impairments[2,3,5], although the neuronal underpinnings sufficient to support behavioural improvements are largely unknown. Here we acutely rescue stress-induced depression-related behaviours in mice by optogenetically reactivating dentate gyrus cells that were previously active during a positive experience. A brain-wide histological investigation, coupled with pharmacological and projection-specific optogenetic blockade experiments, identified glutamatergic activity in the hippocampus–amygdala–nucleus-accumbens pathway as a candidate circuit supporting the acute rescue. Finally, chronically reactivating hippocampal cells associated with a positive memory resulted in the rescue of stress-induced behavioural impairments and neurogenesis at time points beyond the light stimulation. Together, our data suggest that activating positive memories artificially is sufficient to suppress depression-like behaviours and point to dentate gyrus engram cells as potential therapeutic nodes for intervening with maladaptive behavioural states.

Our recent studies have demonstrated that dentate gyrus cells that express c-Fos during fear or reward conditioning define an active neural population that is sufficient to elicit both aversive and appetitive responses, and that the mnemonic output elicited by these artificially reactivated cells can be updated with new information[6–8]. These findings raise the possibility of alleviating stress-induced behavioural impairments via a defined set of dentate gyrus cells that are active during a positive experience. Indeed, how positive episodes interact with psychiatric-disease-related behavioural states, including depression-related impairments, at the neuronal and systems level remains largely unknown, despite the promising cognitive treatments available in humans[9].

To address this issue, we used our recently developed method that enables labelling and manipulation of memory engram cells (see Methods)[6–8]. Exposing animals that were taken off doxycycline to a naturally rewarding experience[8] (that is, exposure to a female mouse in a modified home cage, hereafter referred to as a 'positive experience' and further validated in Extended Data Fig. 1), a neutral context (hereafter referred to as a 'neutral experience'), or a single bout of immobilization stress (hereafter referred to as a 'negative experience') all elicited comparable levels of ChR2–mCherry expression in the dentate gyrus (Extended Data Fig. 2a–e).

As shown in Fig. 1a, mice were split into six groups (see Methods). After 10 days of chronic immobilization stress (CIS) (Extended Data Fig. 2f) or in a home cage, all groups were put through the open field test (OFT) and elevated plus maze test (EPMT) as measures of anxiety-like behaviours, as well as the tail suspension test (TST) as a measure of active/passive escape behaviour in response to a challenging situation, and the sucrose preference test (SPT) for anhedonia[10–14]. In unstressed animals, optogenetic reactivation of cells previously active during a positive experience did not significantly change anxiety-related measures, time spent struggling, or preference for sucrose compared to unstressed mCherry controls (Fig. 1b–e). In the stressed groups, the CIS paradigm elicited a robust decrease in time struggling and preference for sucrose, as well as increased anxiogenic responses, consistent with previous reports[13,14] (Fig. 1b–e).

However, optically reactivating dentate gyrus cells that were previously active during a positive experience, but not a neutral or a negative experience, in stressed animals acutely increased time struggling and sucrose preference to levels that matched the unstressed group's behaviour (Fig. 1b, c). Additionally, optical reactivation of dentate gyrus cells associated with a positive experience decreased the latency to feed in a novelty-suppressed feeding test (NSFT)[14] (Extended Data Fig. 3a) without affecting hunger or satiety (Extended Data Fig. 3b). Once again, the CIS paradigm had an anxiogenic effect across all groups, and all groups failed to show light-induced behavioural changes in the OFT or EPMT (Fig. 1d, e). Similarly, total distance travelled was consistent across groups (Extended Data Fig. 4c). Taken together, these data argue that reactivating dentate gyrus cells labelled by a positive experience is sufficient to acutely reverse the behavioural effects of stress in the TST, SPT and NSFT.

To identify potential neural loci that mediate the light-induced reversal of the stress-induced behaviours observed in our experiments, all subjects first underwent the CIS protocol and then were exposed to the TST while dentate gyrus cells previously active during a positive experience were optically reactivated. We then performed a brain-wide mapping of c-Fos expression in areas activated by this treatment (Fig. 2a).

Optical reactivation of dentate gyrus cells labelled by a positive experience correlated with a robust increase of c-Fos expression in several brain areas, including the nucleus accumbens (NAcc) shell, lateral septum, basolateral amygdala (BLA), central amygdala, as well as the dorsomedial, ventromedial, and lateral hypothalamus (Fig. 2b–i and Extended Data Fig. 5a, b), but not in the medial prefrontal cortex (mPFC) (Fig. 2j–m) or in several other loci (Extended Data Fig. 5c–e). Furthermore, we monitored single-unit activity in the BLA of mice while simultaneously activating dentate gyrus positive memory-engram cells with blue light and found that ~8% of cells (9/106; $n = 3$ mice) had excitatory (8/9 cells) or inhibitory (1/9 cells) responses (Extended Data Fig. 4a). A parallel set of experiments in which unstressed animals received optical stimulation of dentate gyrus cells revealed mostly similar patterns of c-Fos expression (Extended Data Fig. 6).

The NAcc has been heavily implicated in stress responses, mood disorders, and processing natural rewards[2,5,10–12,15–20]. Moreover, pathophysiological dysfunction of the NAcc in response to various stressors has been implicated in anhedonia and reward conditioning[17–20]. Our within-subject experiments revealed that, in the TST, the behavioural

[1]RIKEN-MIT Center for Neural Circuit Genetics at the Picower Institute for Learning and Memory, Department of Biology and Department of Brain and Cognitive Sciences, Massachusetts Institute of Technology, Cambridge, Massachusetts 02139, USA. [2]Howard Hughes Medical Institute, Massachusetts Institute of Technology, Cambridge, Massachusetts 02139, USA. ‡Deceased.

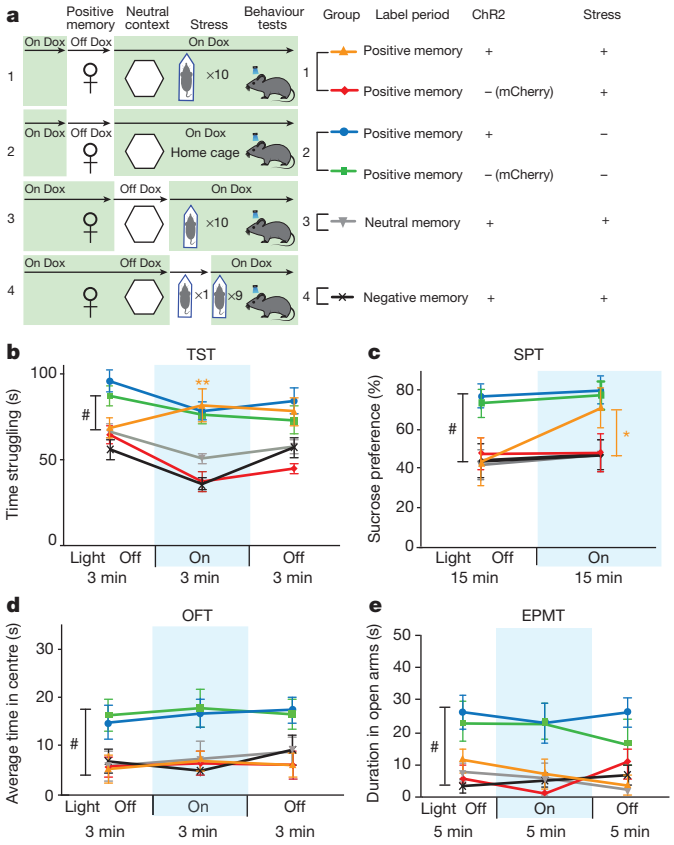

Figure 1 | Activating positive memory engrams rescues depression-related behaviour. **a**, Behaviour schedule and groups used. Dox, doxycycline. Female symbols represent exposure to a female conspecific, white hexagons represent neutral contexts, and mice in the 'stress' condition are depicted undergoing an immobilization protocol. **b**–**e**, Optical reactivation of dentate gyrus cells that were previously active during a positive experience significantly increases time struggling in the tail suspension test (**b**) and preference for sucrose (**c**), but does not have a significant effect in anxiety-like behaviour in the open field test (**d**) or elevated plus maze test (**e**). A two-way analysis of variance (ANOVA) with repeated measures revealed a group-by-light epoch interaction in the TST ($F_{5,294} = 21.20$, $P < 0.001$) or SPT ($F_{5,196} = 6.20$, $P < 0.001$) followed by Bonferroni post hoc tests, which revealed significant increases in struggling or preference for sucrose in the positive memory plus stress group. #$P < 0.01$. # used to denote significant differences between the four stressed groups ($n = 18$ per group) versus the two non-stressed groups ($n = 16$ per group); *$P < 0.05$, **$P < 0.01$ (orange asterisks used to denote significant differences between the stress plus positive memory group versus the other three stressed groups). Data are means ± s.e.m.

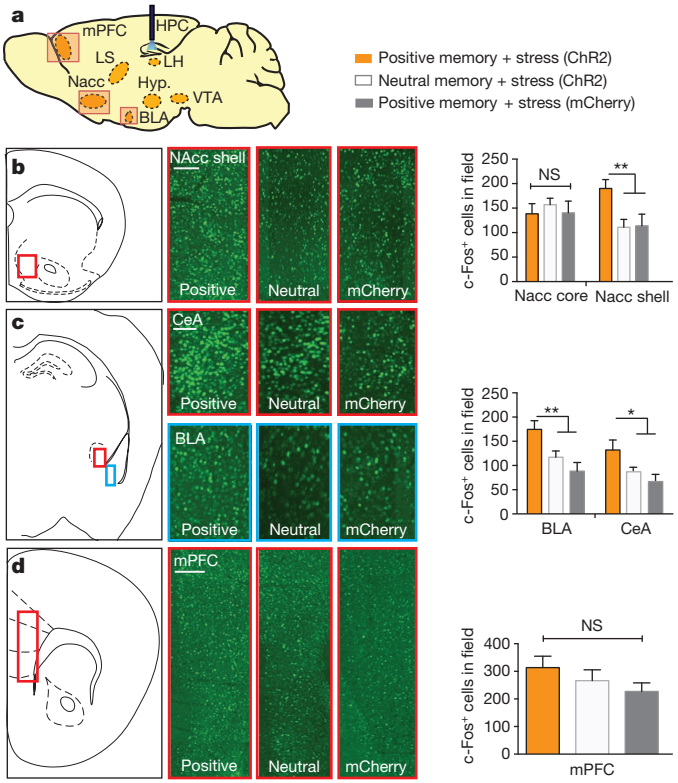

Figure 2 | Positive memory reactivation increases c-Fos expression in the nucleus accumbens shell and the amygdala. **a**, Brain diagram illustrating target areas analysed. **b**–**d**, Activation of a positive memory, but not a neutral memory or mCherry only, in the dentate gyrus during the TST elicits robust c-Fos expression in the nucleus accumbens shell (**b**), basolateral amygdala, and central amygdala (**c**), but not in the medial prefrontal cortex (**d**). For histological data, a one-way ANOVA followed by a Bonferroni post hoc test revealed a significant increase of c-Fos expression in the positive memory plus stress group relative to controls in the NAcc and amygdala, but not the mPFC (NAcc shell, $F_{2,30} = 15.2$, $P < 0.01$; BLA, $F_{2,30} = 11.71$, $P < 0.01$; central amygdala, $F_{2,30} = 11.45$, $P < 0.05$; mPFC, $F_{2,30} = 1.33$, $P = 0.294$. $n = 6$ animals per group, 3–5 slices per animal). NS, not significant; *$P < 0.05$, **$P < 0.01$. Data are means ± s.e.m. Scale bars correspond to 100 μm. HPC, hippocampus; LH, lateral habenula; LS, lateral septum; Hyp., hypothalamus.

effects of optically reactivating dentate gyrus cells labelled by a positive experience were blocked in the group of mice that concurrently received the glutamate receptor antagonists NBQX and AP5 in the NAcc, but not in the group that received saline, without altering basal locomotion (Extended Data Fig. 4b, c). Blocking dopaminergic activity yielded a similar blockade of the dentate gyrus light-induced effects (Extended Data Fig. 7a).

The BLA is known to have robust glutamatergic inputs to the NAcc[19], and previous studies have implicated BLA projections to the NAcc in enabling reward-seeking behaviour[19]. We therefore investigated whether the hippocampus (dentate gyrus)–BLA–NAcc functional pathway is crucial for the real-time light-induced rescue of depression-related behaviour. Our transgenic mice were bilaterally injected with TRE–ArchT–eGFP into the BLA to allow for activity-dependent ArchT–eGFP labelling of axonal terminals from the BLA to the NAcc in response to a positive experience[21] (Fig. 3a, b). Optic fibres were bilaterally placed over the NAcc and the dentate gyrus to allow for real-time inhibition of these terminals originating from ~18% (Fig. 3c) of BLA neurons and simultaneous activation of ChR2–mCherry-positive dentate gyrus cells, respectively, in stressed mice. At the neuronal level, light-induced reactivation of dentate gyrus cells previously activated by a positive experience also reactivated BLA[8] and NAcc[18], but not mPFC, cells (that is, endogenous c-Fos$^+$ cells, red) previously activated by the same positive experience (that is, ArchT–eGFP$^+$ cells, green) (Fig. 3c). These results suggest that the dentate gyrus engram cells are functionally connected to BLA engram cells and NAcc engram cells. At the behavioural level, inhibition of BLA terminals onto the NAcc blocked the dentate gyrus light-induced rescue in both the TST and SPT (Fig. 3d–g). Within the same behavioural session for the TST, and across 2 days for the SPT, when ArchT-mediated inhibition was released (that is, the green light was turned off), the rescue effects of reactivating dentate gyrus cells previously active during a positive experience were rapidly observed in all groups (Fig. 3d–g). ArchT-mediated inhibition of BLA–NAcc terminals alone did not negatively affect behaviour in the TST or SPT beyond the levels of the stressed animals (Fig. 3d–g insets). The specificity of the hippocampus (dentate gyrus)–BLA–NAcc pathway for the rescue was supported by an analogous experiment conducted with bilateral injections of TRE–ArchT–eGFP into the mPFC. Although the mPFC is also known to provide robust glutamatergic input to the NAcc[19], the induction of c-Fos expression in this area upon optogenetic activation of dentate gyrus cells associated with a positive experience was not significantly higher

than that observed with a neutral experience (Fig. 2m), and mPFC cells reactivated by dentate gyrus cell reactivation was at chance level (Fig. 3c). Correspondingly, inhibition of terminals originating from ~12% of the mPFC (Fig. 3c) onto the NAcc did not block the dentate gyrus light-induced rescue in either the TST or SPT (Fig. 3d–g). Moreover, inhibition of BLA, but not mPFC, terminals onto the NAcc partially inhibited the dentate-gyrus-mediated, light-induced increase of c-Fos$^+$ cells observed in the NAcc shell (Fig. 3h), supporting the conclusion that the hippocampal (dentate gyrus)–BLA–NAcc pathway of positive engrams plays a crucial role in the rescue of depression-related behavioural phenotypes.

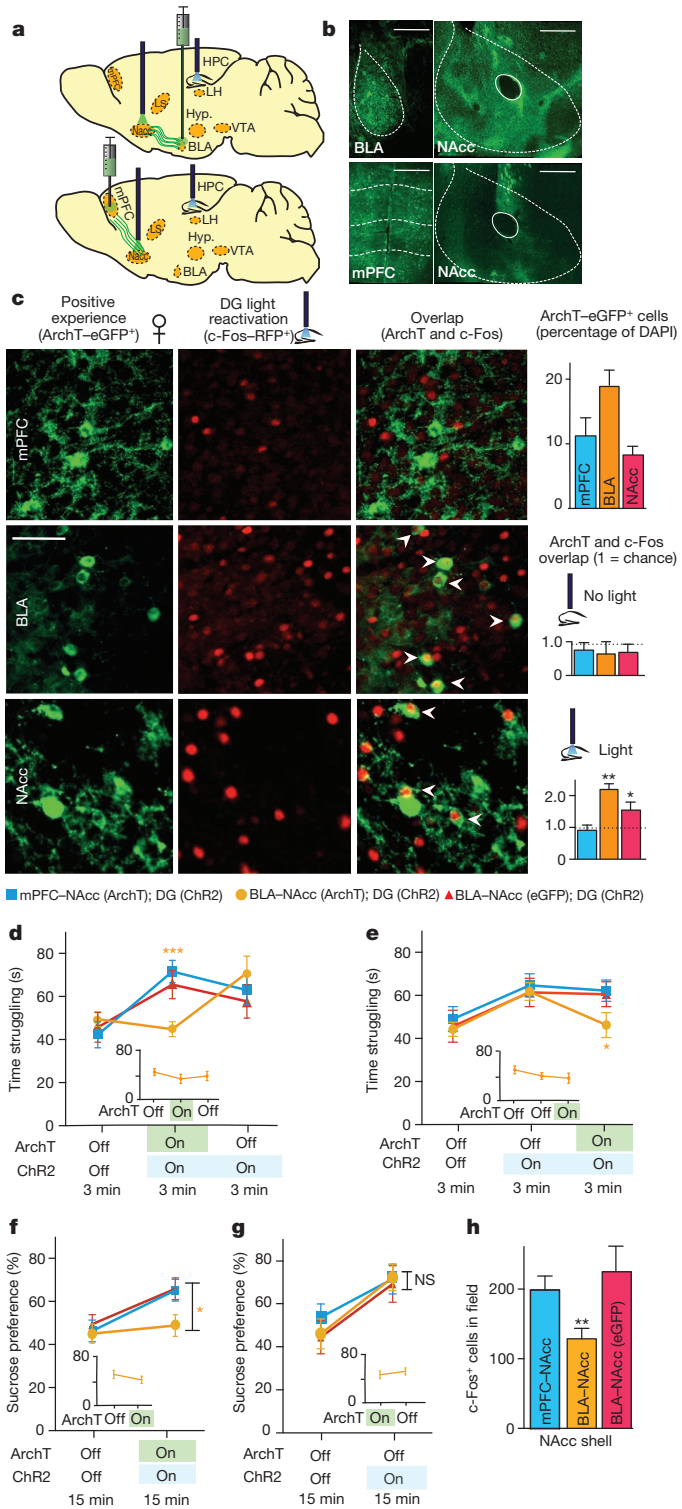

Recent meta-analyses have suggested that treating psychiatric disorders through prescribed medication or cognitive interventions are capable of producing symptom remission when administered chronically[20], though the neural underpinnings inducing and correlating with long-lasting rescues are poorly understood[20,22,23]. The aforementioned acute intervention did not induce enduring behavioural changes (Extended Data Fig. 7b). We therefore investigated whether chronic reactivation of dentate gyrus engram cells could attenuate depression-related behaviours in a manner that outlasted acute optical stimulation following the protocol depicted in Fig. 4a (Methods). A group in which dentate gyrus cells associated with a positive experience were optically reactivated across 5 days, but not 1-day or no stimulation groups, showed a reversal of the stress-induced behavioural deficits measured in the TST and SPT that was not significantly different from an unstressed control group (Fig. 4b, c). A group in which dentate gyrus cells associated with a neutral experience were optically reactivated across 5 days did not show such effects, nor did a group that was exposed to a natural social reward for 5 days (Fig. 4b–d). Histological analyses revealed decreased levels of neurogenesis as measured both by the polysialylated neuronal cell adhesion molecule (PSA-NCAM) and doublecortin (DCX)—often considered markers of developing and migrating neurons[24,25]—in all stressed groups except for the positive experience and 5-day stimulation group, and the unstressed control group (Fig. 4d and Extended Data Fig. 8). This increase in adult-born neurons positively correlated with the degree to which each group preferred sucrose in the SPT (Extended Data Fig. 9a); moreover, performance levels on the SPT and TST positively correlated with one another on an animal-by-animal basis (Extended Data Fig. 9b).

Our data demonstrate that the depression-related readouts of active/passive coping-like behaviour and anhedonia, as measured in the TST and SPT, respectively, can be ameliorated by activating cells in the hippocampus associated with a positive memory, while anxiety-related behaviours measured by the OFT and EPMT remained unchanged. Differential regulation of depression- and anxiety-related behaviour could have been achieved by leveraging the functional

Figure 3 | The antidepressant effects of an optically activated positive memory require real-time terminal activity from the BLA to the NAcc. **a**, Brain diagram illustrating target areas manipulated. **b**, Representative coronal slices showing TRE–ArchT–eGFP-positive cells in the BLA or mPFC, as well as their corresponding terminals in the NAcc. Scale bars: BLA and mPFC, 500 μm; NAcc, 200 μm. **c**, Animals were taken off Dox and initially exposed to a positive experience, which caused labelling of corresponding BLA (~18%), mPFC (~12%), or NAcc (~9%) cells with eGFP derived from AAV_9-TRE-ArchT-eGFP (green, halo-like expression). Light-activation of a positive memory engram in the dentate gyrus (DG) preferentially reactivated the BLA and NAcc shell cells, as measured by endogenous c-Fos expression (red, nucleus-localized), that were originally labelled by the same positive experience, while groups with no light stimulation showed levels of overlap not significantly different from chance. Arrowheads indicate double-stained cells. Scale bar, 5 μm. **d**–**g**, ArchT-mediated inhibition of BLA, but not mPFC, terminals in the NAcc prevents the dentate-gyrus-mediated light-induced increases in struggling (**d**, **e**) or preference for sucrose (**f**, **g**), while inhibition of BLA terminals in the NAcc without dentate gyrus stimulation does not affect behaviour (insets). **h**, ArchT-mediated inhibition of BLA, but not mPFC, terminals prevents the dentate-gyrus-mediated light-induced increase of c-Fos expression in the NAcc. For behavioural data, a two-way ANOVA with repeated measures followed by a Bonferroni post hoc test revealed a group-by-light epoch interaction and significant ArchT-mediated attenuation of struggling in the TST (**d**: $F_{2,99} = 7.30$, $P < 0.001$; **e**: $F_{2,99} = 6.61$, $P < 0.01$) or preference for sucrose water in the the SPT (**f**: $F_{2,66} = 10.66$, $P < 0.01$). $n = 12$ per behavioural group. $^*P < 0.05$, $^{**}P < 0.01$, $^{***}P < 0.001$; orange asterisks used to denote significant differences between the stress plus positive memory group versus all other groups. For histological data, one-sample t-tests against chance overlap were performed ($n = 4$ per group, 3–5 slices per animal). NS, not significant. HPC, hippocampus; LH, lateral habenula; LS, lateral septum; Hyp., hypothalamus. Data are means ± s.e.m.

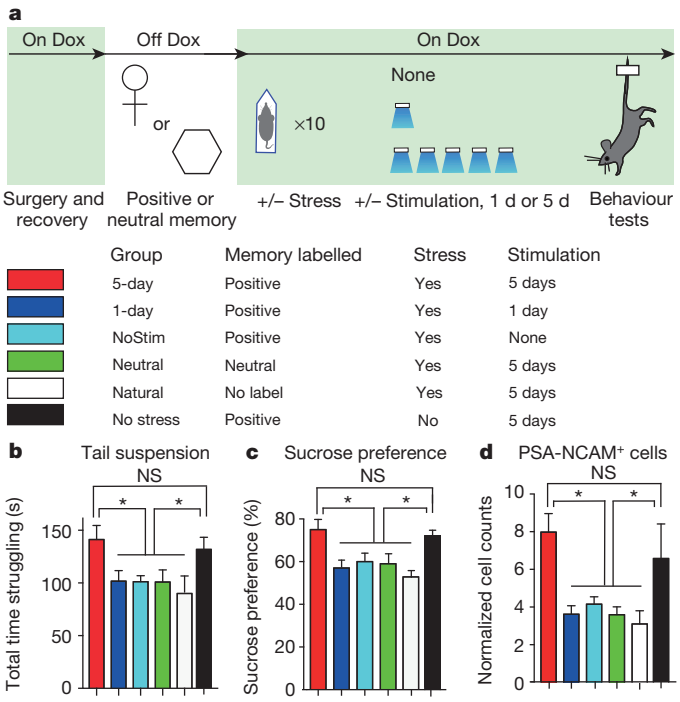

Figure 4 | Chronic activation of a positive memory elicits a long-lasting rescue of depression-related behaviour. **a**, Behavioural schedule and groups used. NoStim, no stimulation. Female symbols represent exposure to a female conspecific, white hexagons represent neutral contexts, and mice in the 'stress' condition are depicted undergoing an immobilization protocol. **b**, **c**, Animals in which a positive memory was reactivated twice a day for 5 days showed increased struggling in a 6-min tail suspension test ($F_{5,78} = 3.34$, $P < 0.05$) (**b**) and increased preference for sucrose measured over 24 h ($F_{5,84} = 6.25$, $P < 0.01$) (**c**). **d**, The 5-day positive memory stimulation group showed a significant increase of adult newborn cells in the dentate gyrus as measured by PSA-NCAM$^+$ cells ($F_{5,72} = 4.65$, $P < 0.01$; see Extended Data Fig. 8 for doublecortin data and PSA-NCAM images). For these data (**b**–**d**), a one-way ANOVA revealed a significant interaction of the experimental-group factor and stimulation-condition factor and was followed by a Bonferroni post hoc test. $n = 14$ per TST behavioural group, $n = 15$ per SPT behavioural group, $n = 5$ slices per animal for data appearing in **d**. *$P < 0.05$. Data are means ± s.e.m.

segregation present along the hippocampus dorsal–ventral axis; for instance, activation of ventral hippocampal dentate gyrus engram cells could reveal heterogeneous, behaviourally relevant roles in the emotional regulation of anxiety and stress responses that our dorsal hippocampus manipulations presumably did not access[26,27]. To that end, we speculate that, at the engram level, the circuitry sufficient to modulate anxiety-related behaviour relies more heavily on a synaptic dialogue within the amygdala, its bidirectional connections with the ventral hippocampus, and its effects on downstream mesolimbic and cortical structures[10,11,26,27].

Depression is diagnosed as a constellation of heterogeneous symptoms; their complex aetiology and pathophysiology underscore the varied responses to currently available treatments. While most psychopharmacological treatments take weeks to achieve effects, other alternative treatments such as deep-brain stimulation and the NMDA antagonist ketamine have been reported to have rapid effects in a subset of patients[28]. In rodents, optogenetic stimulation of mPFC neurons, mPFC to raphe projections, and ventral tegmental dopaminergic neurons achieved a rapid reversal of stress-induced maladaptive behaviours[4,10,11]. We speculate that our acute behavioural changes reflect the degree to which directly stimulating positive-memory-engram-bearing cells might bypass the plasticity that normally takes antidepressants weeks or months to achieve, thereby temporarily suppressing the depression-like state. In support, we observed that the effects of optically stimulating a positive memory are contingent on active glutamatergic projections from the amygdala to the NAcc in real time, as well as intra-NAcc dopamine activity[18]. Our data dovetail with this circuit's proposed role of relaying BLA stimulus-reward associations to a ventral striatal motor-limbic interface. This interface is thought to be capable of coalescing such information with motivational states and finally translating such activity into behaviourally relevant outputs[5,17–19].

Moreover, our chronic stimulation data reveal that repeatedly activating dentate gyrus engram cells associated with a positive experience elicits an enduring reversal of stress-induced behavioural abnormalities and an increase in neurogenesis. While future experiments are required to identify the causal link between chronically reactivated positive memory engrams and the corresponding rescue of behaviours, many tantalizing hypotheses surface, including a normalization of VTA firing rates[29], epigenetic and differential modification of effector proteins (for example, CREB, BDNF) in areas upstream and downstream of the hippocampus[30], and a reversal of neural atrophy in areas such as CA3 and mPFC or hypertrophy in BLA[26]. The aforementioned molecular and homeostatic mechanisms—in addition to our observed increase of adult-born neurons in the 5-day stimulation group—could be partly realized in a hormone- or neuromodulator-mediated manner (Extended Data Fig. 5). Finally, our data demonstrate that exposing stressed subjects to a natural positive experience repeatedly is not effective, while repeated direct reactivations of dentate gyrus engram cells associated with a previously acquired positive memory is effective (Fig. 4b–d). We speculate that invasively stimulating these dentate gyrus cells is effective in activating both the internal contextual representation associated with a positive experience as well as associated downstream areas, while exposure to natural exogenous positive cues may not be able to access similar neural pathways in subjects displaying depression-like symptoms such as passive behaviour in challenging situations and anhedonia (Fig. 4b–d).

Collectively, the data described here build a novel experimental bridge between memory engrams in the brain and animal models of psychiatric disorders. We propose that direct activation of dentate gyrus engram cells associated with a positive memory offers a potential therapeutic node for alleviating a subset of depression-related behaviours and, more generally, that directly activating endogenous neuronal processes may be an effective means to correct maladaptive behaviours.

Online Content Methods, along with any additional Extended Data display items and Source Data, are available in the online version of the paper; references unique to these sections appear only in the online paper.

Received 14 October 2014; accepted 1 May 2015.

1. Caspi, A. *et al.* Influence of life stress on depression: moderation by a polymorphism in the 5-HTT gene. *Science* **301,** 386–389 (2003).
2. Pittenger, C. & Duman, R. S. Stress, depression, and neuroplasticity: a convergence of mechanisms. *Neuropsychopharmacology* **33,** 88–109 (2008).
3. Hyman, S. E. Revitalizing psychiatric therapeutics. *Neuropsychopharmacology* **39,** 220–229 (2014).
4. Covington, H. E. III *et al.* Antidepressant effect of optogenetic stimulation of the medial prefrontal cortex. *J. Neurosci.* **30,** 16082–16090 (2010).
5. Russo, S. J. & Nestler, E. J. The brain reward circuitry in mood disorders. *Nature Rev. Neurosci.* **14,** 609–625 (2013).
6. Liu, X. *et al.* Optogenetic stimulation of a hippocampal engram activates fear memory recall. *Nature* **484,** 381–385 (2012).
7. Ramirez, S. *et al.* Creating a false memory in the hippocampus. *Science* **341,** 387–391 (2013).
8. Redondo, R. L. *et al.* Bidirectional switch of the valence associated with a hippocampal contextual memory engram. *Nature* **513,** 426–430 (2014).
9. Seligman, M. E. P., Rashid, T. & Parks, A. C. Positive psychotherapy. *Am. Psychol.* **61,** 774–788 (2006).
10. Tye, K. M. *et al.* Dopamine neurons modulate neural encoding and expression of depression-related behaviour. *Nature* **493,** 537–541 (2013).
11. Warden, M. R. *et al.* A prefrontal cortex-brainstem neuronal projection that controls response to behavioural challenge. *Nature* **492,** 428–432 (2012).
12. Deisseroth, K. Circuit dynamics of adaptive and maladaptive behaviour. *Nature* **505,** 309–317 (2014).

13. Lim, B. K., Huang, K. W., Grueter, B. A., Rothwell, P. E. & Malenka, R. C. Anhedonia requires MC4R-mediated synaptic adaptations in nucleus accumbens. *Nature* **487,** 183–189 (2012).
14. Snyder, J. S., Soumier, A., Brewer, M., Pickel, J. & Cameron, H. A. Adult hippocampal neurogenesis buffers stress responses and depressive behaviour. *Nature* **476,** 458–461 (2011).
15. Lammel, S. *et al.* Input-specific control of reward and aversion in the ventral tegmental area. *Nature* **491,** 212–217 (2012).
16. Dölen, G., Darvishzadeh, A., Huang, K. W. & Malenka, R. C. Social reward requires coordinated activity of nucleus accumbens oxytocin and serotonin. *Nature* **501,** 179–184 (2013).
17. Schlaepfer, T. E. *et al.* Deep brain stimulation to reward circuitry alleviates anhedonia in refractory major depression. *Neuropsychopharmacology* **33,** 368–377 (2008).
18. Xiu, J. *et al.* Visualizing an emotional valence map in the limbic forebrain by TAI-FISH. *Nature Neurosci.* **17,** 1552–1559 (2014).
19. Stuber, G. D. *et al.* Excitatory transmission from the amygdala to nucleus accumbens facilitates reward seeking. *Nature* **475,** 377–380 (2011).
20. DeRubeis, R. J., Siegle, G. J. & Hollon, S. D. Cognitive therapy versis medication. *Nature Rev. Neurosci.* **9,** 788–796 (2008).
21. Han, X. *et al.* A high-light sensitivity optical neural silencer: development and application to optogenetic control of non-human primate cortex. *Front. Syst. Neurosci.* **5,** 18 (2011).
22. Brody, A. L. *et al.* Regional brain metabolic changes in patients with major depression treated with either paroxetine or interpersonal therapy. *Arch. Gen. Psychiatry* **58,** 631–640 (2001).
23. Airan, R. D. *et al.* High-speed imaging reveals neurophysiological links to behavior in an animal model of depression. *Science* **317,** 819–823 (2007).
24. Seki, T. & Arai, Y. Highly polysialylated neural cell adhesion molecule (NCAM-H) is expressed by newly generated granule cells in the dentate gyrus of the adult rat. *J. Neurosci.* **13,** 2351–2358 (1993).
25. Santarelli, L. *et al.* Requirement of hippocampal neurogenesis for the behavioral effects of antidepressants. *Science* **301,** 805–809 (2003).
26. Roozendaal, B., McEwen, B. S. & Chattarji, S. Stress, memory and the amygdala. *Nature Rev. Neurosci.* **10,** 423–433 (2009).
27. Felix-Ortiz, A. C. *et al.* BLA to vHPC inputs modulate anxiety-related behaviors. *Neuron* **79,** 658–664 (2013).
28. Berman, R. M. *et al.* Antidepressant effects of ketamine in depressed patients. *Biol. Psychiatry* **47,** 351–354 (2000).
29. Friedman, A. K. *et al.* Enhancing depression mechanisms in midbrain dopamine neurons achieves homeostatic resilience. *Science* **344,** 313–319 (2014).
30. Tsankova, N., Renthal, W., Kumar, A. & Nestler, E. J. Epigenetic regulation in psychiatric disorders. *Nature Rev. Neurosci.* **8,** 355–367 (2007).

Acknowledgements We thank B. Chen, D. S. Roy, and J. Kim for help with the experiments, T. J. Ryan and T. Kitamura for the TRE–ArchT–eGFP construct, J. Sarinana and E. Hueske for comments and extensive discussions on the manuscript, and all the members of the Tonegawa laboratory for their support. We dedicate this study to the memory of Xu Liu, who made major contributions to memory engram research. This work was supported by RIKEN Brain Science Institute and Howard Hughes Medical Institute.

Author Contributions S.R., X.L., C.M., A.M., J.Z., R.L.R. and S.T. contributed to the study design. S.R., X.L., A.M., J.Z., C.M. and R.L.R. contributed to the data collection and interpretation. X.L. cloned all constructs. S.R., X.L., C.M., J.Z. and A.M. conducted the surgeries, behaviour experiments, and histological analyses. S.R., X.L. and S.T. wrote the paper. All authors discussed and commented on the manuscript.

Author Information Reprints and permissions information is available at www.nature.com/reprints. The authors declare no competing financial interests. Readers are welcome to comment on the online version of the paper. Correspondence and requests for materials should be addressed to S.T. (tonegawa@mit.edu).

METHODS

Subjects. The *c-fos-tTA* mice were generated by crossing TetTag[31] mice with C57BL/6J mice and selecting for those carrying the *c-fos-tTA* transgene. Littermates were housed together before surgery and received food and water *ad libitum*. All mice were raised on a diet containing 40 mg kg^{-1} doxycycline (Dox) for a minimum of 1 week before receiving surgery at age 12–16 weeks. Post-operation, mice were individually housed in a quiet home cage with a reverse 12 h light–dark cycle, given food and water *ad libitum*, and allowed to recover for a minimum of 2–3 weeks before experimentation. All animals were taken off Dox for an undisturbed 42 h to open a time window of activity-dependent labelling. In our system, the promoter of c-Fos—an immediately early gene often used as a marker of recent neural activity—is engineered to drive the expression of the tetracycline transactivator (tTA), which in its protein form binds to the tetracycline response element (TRE). Subsequently, the activated TRE drives the light-responsive channelrhodopsin-2 (ChR2). Importantly, the expression of ChR2 only occurs in the absence of doxycycline (Dox) from the animal's diet, thus permitting inducible expression of ChR2 in correspondingly active cells.

Each group of male mice was exposed to all three subsequent treatments for 2 hours and randomly assigned which experience would occur while off Dox; a negative experience (that is, a single bout of immobilization stress, see below), a naturally rewarding experience (that is, exposure to a female conspecific while in a modified home cage, as previously reported[32]), and a neutral experience (that is, exposure to a conditioning chamber). For female exposure, single-caged male mice were moved to a behaviour room distinct from the housing room and with dim lighting conditions. Next, the cage tops were removed and a 4-sided (31 × 25 × 30 cm) white box was placed over the home cage, after which a female mouse was introduced to the home cage. Importantly, this modification to the home cage during female exposure ensured similar levels of dentate gyrus labelling as the neutral and negative memory exposure groups (Extended Data Fig. 2). Each group was taken off Dox only during one of the aforementioned treatments and placed back on Dox immediately afterwards. The subjects were age-matched and split into two groups: a stressed group and a non-stressed group. Non-stressed animals remained in their home cages before experimentation. Stressed animals underwent 2–3 h of chronic immobilization stress (CIS) each day for ten consecutive days before behavioural testing using Mouse DecapiCone disposable restrainers. All procedures relating to mouse care and treatment conformed to the institutional and National Institutes of Health guidelines for the Care and Use of Laboratory Animals. Sample sizes were chosen on the basis of previous studies[32–34]; variance was similar between groups for all metrics measured. No statistical methods were used to predetermine sample size.

Virus constructs and packaging. The $pAAV_9$-TRE-ChR2-mCherry and $pAAV_9$-TRE-mCherry plasmids were constructed as previously reported[33]. The $pAAV_9$-TRE-ArchT-eGFP was constructed by replacing the *ChR2-eYFP* fusion gene in the $pAAV_9$-TRE-ChR2-eYFP plasmid from Liu *et al.*[34] with a fusion gene of *ArchT-eGFP* from Han *et al.*[35]. These plasmids were used to generate AAV_9 viruses by the Gene Therapy Center and Vector Core at the University of Massachusetts Medical School. Viral titrations were 8×10^{12} genome copy per ml for AAV_9-TRE-ChR2-mCherry, 1.4×10^{13} genome copy per ml for AAV_9-TRE-mCherry, and 0.75 to 1.5×10^{13} genome copy per ml for AAV_9-TRE-ArchT-eGFP.

Stereotactic injection, cannulation, and fibre optic implants. All surgeries were performed under stereotaxic guidance and subsequent coordinates are given relative to bregma. Animals were anaesthetized using 500 mg kg^{-1} Avertin before receiving bilateral craniotomies using a 0.5 mm diameter drill bit at −2.2 mm anterioposterior (AP), ±1.3 mm mediolateral (ML) for dentate gyrus injections. All mice were injected with 0.15 µl of AAV9 virus at a controlled rate of 0.6 µl min^{-1} using a mineral oil-filled glass micropipette joined by a microelectrode holder (MPH6S; WPI) to a 10 µl Hamilton microsyringe (701LT; Hamilton) in a microsyringe pump (UMP3; WPI). The needle was slowly lowered to the target site at −2.0 mm dorsoventral (DV). The micropipette remained at the target site for another 5 minutes post-injection before being slowly withdrawn. A bilateral optical fibre implant (200 µm core diameter; Doric Lenses) was lowered above the injection site (−1.6 mm DV for dentate gyrus) and three jewellery screws were secured into the skull at the anterior and posterior edges of the surgical site to anchor the implant. For mice used in pharmacological manipulations, bilateral guide cannula (PlasticsOne) were implanted above the NAcc (+1.2 mm AP; ±0.5 mm ML; −3.25 mm DV). Mice used in the BLA-to-NAcc or mPFC-to-NAcc experiments received bilateral injections (0.2 µl to 0.3 µl) of TRE-ArchT-eGFP or TRE-eGFP into the BLA (−1.46 mm AP; ±3.20 mm ML; −4.80 mm DV), NAcc (+1.2 mm AP; ±0.50 mm ML; −4.3 mm DV), or the mPFC (+1.70 mm AP; ±0.35 mm ML; −2.70 mm DV). These mice were then injected with TRE–ChR2–mCherry into the dentate gyrus and received bilateral optic fibre implantation as described above (Doric Lenses), as well as bilateral optic fibre implantation over the NAcc (+1.2 mm AP; ±0.50 mm ML; −3.70 mm DV).

Layers of adhesive cement (C&B Metabond) followed by dental cement (Teets cold cure; A-M Systems) were spread over the surgical site and protective cap to secure the optical fibre implant. The protective cap was made from the top portion of a black polypropylene microcentrifuge tube. Mice received intraperitoneal injections of 1.5 mg kg^{-1} analgesics and were placed on heating pads throughout the procedure until recovery from anaesthesia. Histological studies were used to verify fibre placements and viral injection sites. Only data from mice with opsin or fluorophore expression restricted to the dentate gyrus, BLA or mPFC were used for histological, behavioural and statistical analyses.

Pharmacological infusion of glutamate or dopamine receptor antagonists. Glutamate antagonists were bilaterally infused into the NAcc as follows: 0.2 µl per hemisphere of NBQX at a concentration of 22.3 mM to antagonize AMPA (α-amino-3-hydroxy-5-methyl-4-isoxazole propionic acid) receptors and 0.2 µl per hemisphere of AP5 at a concentration of 38.04 mM to antagonize NMDA (*N*-methyl-D-aspartate) receptors. Dopamine receptor antagonists were bilaterally infused into the NAcc as follows: 0.2 µl SCH23390 at a concentration of 6.16 mM to antagonize D1-like receptors and 0.2 µl raclopride at a concentration of 2.89 mM to antagonize D2-like receptors. A 26-gauge stainless steel double internal cannula (PlasticsOne) was used to bilaterally infuse each drug; the internal cannula was connected with a microsyringe pump by a PE20 tube to control the injection rate at 100 nl min^{-1}. The injection cannula was left connected for 5 min before removal to allow for diffusion. Finally, all behaviour was performed 20 min following drug infusion.

Immunohistochemistry. Mice were overdosed with 750–1000 mg kg^{-1} Avertin and perfused transcardially with cold PBS, followed by 4% paraformaldehyde (PFA) in PBS. Extracted brains were kept in 4% PFA at 4 °C overnight, then transferred to PBS. A vibratome was used to recover 50-µm coronal slices in cold PBS. Slices were washed with PBS-T (PBS + 0.2% Triton X-100), then incubated with PBS-T + 5% normal goat serum at 4 °C for 1 h for blocking. For immunostaining, slices were incubated with one or more primary antibodies (1:1000 dilution) at 4 °C for 24 h (600-401-379 Rockland; A10262, Invitrogen; SC-52, Santa Cruz). Three washes of PBS-T for 10 min each were performed on the slices before 1 h incubation with secondary antibody at 1:200 dilution (A11039, Invitrogen; A21429, Invitrogen). Slices were washed three more times in PBS-T for 10 min each, stained with 4′,6-diamidino-2-phenylindole (DAPI; 1:10,000 dilution) to label cell nuclei and mounted with Vectashield H-1200 onto microscope slides.

Behavioural assays. All behaviour assays were conducted during the light cycle of the day (7:00–19:00) on animals 12–16 weeks old. Mice were handled for 3–5 days, 2 min per day, before all behavioural experiments.

Tail suspension test. Fibre optic implants on experimental mice were plugged into a patch cord before the tail suspension test. Each subject was hung by its tail from a bar 40 cm from the ground with a single piece of autoclave tape. The animal was positioned such that it had no contact with other objects. Immediately after positioning, video recordings of the animal's movements were taken (Noldus by Ethovision). Blue light stimulation was given at 20 Hz, 15 ms pulse width, ~15–20 mW. For behavioural data appearing in Fig. 1, all mice were exposed to a 9 min tail suspension test with light stimulation occurring at minutes 3–5, inclusive; for histological data appearing in Fig. 2, all mice were exposed to a 6 min tail suspension test with light stimulation occurring throughout the entire session using the same stimulation parameters described above. For data appearing in Fig. 3, all animals were given a 9 min tail suspension test once a day for 2 days to assess the effects of ArchT inhibition on BLA or mPFC terminals in the NAcc while simultaneously activating ChR2-positive cells in the dentate gyrus. For half of the subjects, on day 1, ArchT-mediated inhibition occurred during minutes 3–5, inclusive, using constant green light at ~25 mW; dentate gyrus stimulation occurred from minutes 3–8, inclusive. For the other half, ArchT-mediated inhibition occurred during minutes 6–8, inclusive; and dentate gyrus stimulation occurred from minutes 3–8, inclusive. The treatments occurring on days 1 and 2 were counterbalanced within and across groups. A separate cohort of animals were used for the data appearing in the insets of Fig. 3d–g. These groups contained TRE–ChR2–mCherry in the dentate gyrus, as well as bilateral optic fibres over the dentate gyrus, and TRE–ArchT–eGFP in the BLA, as well as optic fibres over the NAcc to inhibit BLA terminals during the appropriate light-on epochs in the TST and SPT. These cohorts, too, were counterbalanced across sessions and only received green light over the NAcc for 3 min during the TST or 15 min during the SPT. For the c-Fos counts appearing in Fig. 3h, all groups underwent a 6 min tail suspension test with blue light delivered to the dentate gyrus and green light delivered to the NAcc throughout the entirety of the session. These groups were sacrificed 1.5 h later for histological analyses. For data appearing in Fig. 4, mice were exposed to a 6 min tail suspension test without light stimulation. An experimenter blind to each mouse condition and light treatment scored all the tail

suspension videos by measuring the total time in seconds that each mouse spent struggling throughout the protocol.

Sucrose preference test. A Med Associates operant chamber—equipped with photolickometers placed on two separate corners of the chamber—was used to count the number of licks made by the mice on lick spouts with direct access to 2% sucrose water solution or water alone. All animals undergoing the sucrose preference protocol were water-restricted for 36 h before each habituation session. These sessions consisted of first plugging the optic fibres on the water-deprived mice to a corresponding patch cord and exposing the mice to the operant chamber, which contained bottles filled only with water. Each exposure occurred on three separate days for 30 min per day. The three habituation sessions occurred interspersed throughout the 10-day chronic immobilization stress protocol (that is, on days 1, 4 and 7 of stress) at least 6 h before or after the stress protocol. In pilot experiments, ~90% of water-deprived animals failed to sample both photolickometers in the operant chamber even after multiple 30-min habituation sessions (data not shown); to address this issue, a glove box was inserted on its side in the operant chamber such that each subject had a narrow ~10 cm corridor to explore and find each lick spout. With this modification, >90% of animals found both lick spouts during the first and subsequent habituation sessions. Upon completing a habituation session, mice were given water only when 2 h of being placed back into the home cage had elapsed. On the test day (that is, the day on which optical stimulation occurred), the location of each sucrose or water bottle in the chamber was counterbalanced between animal chambers. A 30 min protocol—15 min light off, 15 min light on—was used on all animals. The first 15 min were used to detect the baseline preference; blue light stimulation at 20 Hz, 15 ms pulse width, ~15–20 mW, occurred during the second 15 min epoch to detect light-induced changes in preference. For data appearing in Fig. 3, water-deprived animals were exposed to the same 30-min protocol on two separate days. On day 1, after the first 15-min epoch, half of the animals received constant green light stimulation at ~15 mW (as previously reported[36]) over the NAcc while simultaneously receiving blue light stimulation over the dentate gyrus; the other half received only blue light stimulation over the dentate gyrus. On day 2, the treatments were reversed in a counterbalanced manner. Data was only collected in animals that licked at both spouts in the first 15-min interval; animals that did not discover both lick spouts (as evidenced by licking only one spout during the first 15-min interval) were not given light stimulation, the experiment was terminated early, and the test was repeated the following day. Sucrose preferences were calculated as follows:

$$\frac{\text{total number of licks to sucrose spout}}{\text{total number of licks to sucrose spout} + \text{total number of licks to water spout}} \times 100.$$

For the sucrose preference data appearing in Fig. 4, mice were first habituated to two water bottles for 2 days in their home cages. On day 3, two water bottles containing either 2% sucrose or water were placed into the cages in a counterbalanced manner and left undisturbed for 24 h. Sucrose preferences were calculated as follows:

$$\frac{\Delta\text{weight of sucrose water}}{\Delta\text{weight of sucrose water} + \Delta\text{weight of water}} \times 100.$$

Open field test. An open, metal chamber (Accuscan system) with transparent, plastic walls was used for the open field test. Implanted mice were plugged into a patch cord, individually placed into the chamber, and allowed to explore freely for 12 min. An automated video-tracking system (Ethovision by Noldus) was used to track the amount of time spent in the centre of the chamber compared to the edges, as well as the total distance travelled across a session. Light stimulation, as described above, was given during minutes 3–5 and 9–11, inclusive.

Elevated plus maze test. Implanted animals were plugged into a corresponding patch cord before the beginning of the session and subsequently placed in an elevated plus maze. Two pieces of plastic (30 cm long, 5 cm wide) formed the two arms of the maze that intersected at right angles. One arm was enclosed with plastic black walls, and the other arm was open with no walls. The structure was elevated 60 cm above the floor and mice were placed one at a time at the intersection of the maze facing into an arm with walls to start a trial. Video tracking software (EthoVision by Noldus) was used to track the amount of time the mice spent in the enclosed versus the open arms of the maze throughout a 15-min session. Optical stimulation occurred only during the second 5-min epoch using the same stimulation parameters as noted above.

Novelty-suppressed feeding. The novelty suppressed feeding paradigm was performed as previously described[37]. In brief, food was removed from the subjects' home cages 24 h before testing. The next day, mice were placed for 10 min in an open field apparatus containing bedding with a food pellet at the centre on a 1 cm^2 elevated platform. Light stimulation using the parameters described above occurred throughout the entire session. All behaviour was videotaped (Ethovision by Noldus) and latency to feed was scored offline by an experimenter blind to the experimental conditions for each mouse. Once placed back into their home cages, mice were given a single food pellet, which was weighed before and after a 5-min test to measure for motivation/hunger effects on feeding behaviour compared to feeding in a novel environment.

5-day stimulation protocol. For data appearing in Fig. 4, animals were first split into six groups: a group in which dentate gyrus cells previously active during a positive experience were reactivated twice a day for 5 days (5-day group) after the CIS protocol, a group in which such stimulation occurred twice a day for 1 day (1-day group) after the CIS protocol, a group in which no stimulation was delivered (NoStim group) after the CIS protocol, a group in which dentate gyrus cells previously active during a neutral experience were reactivated twice a day for 5 days (Neutral group) after the CIS protocol, a group that did not receive the CIS stress protocol but still had dentate gyrus cells previously active during a positive experience reactivated twice a day for 5 days (NoStress group), and finally, a group that was exposed to a natural social reward (that is, female mouse) twice a day for 5 days (Natural group). Optical stimulation first occurred at 10:00 for 15 min (blue laser, 20 Hz, 15 ms pulse width, ~15–20 mW) as animals explored an operant chamber, and then again at 15:00 for 15 min using the same conditions. The same behavioural schedule was performed for the Natural group. All groups were exposed for an equal amount of time to each chamber, plugged into a corresponding patch cord, and optical stimulation occurred only in the appropriate groups. Each chamber contained dim lighting, white plastic floors, and no artificial odorants. One day after the final stimulation, all groups were exposed to a 6 min tail suspension or 24 h sucrose preference test as described above.

Object–female association. Twenty-four wild-type B6 mice were divided in two groups (neutral-object group, that is, control group, and female-object group, that is, experimental group ($n = 12$ per group)). The learning and testing phases were conducted on the same day, 6 h apart. In the learning phase, all mice spent 30 min in their home cage in the middle of a well-lit room with the lid of the cage and metal grid holding water and food removed and a 30 cm tall white rectangular frame placed around the home cage to prevent mice from escaping. All the boxes contained one target object (counterbalanced objects within and between groups: empty methanol bottle or cryostat liquid bottle (sealed)). After 3 min exploring the target object, a wild-type female b6 mouse (age 9 to 16 weeks) was introduced in the boxes of the experimental mice and remained there for the next 27 min). The control mice did not experience a female mouse and only experienced the object. After a total of 30 min from the beginning of the learning phase, the object and female mouse were removed and the male mice returned to their holding rooms. In the testing phase, mice were placed in a rectangular arena (70 × 25 × 30 cm) with white floors. A video camera resides above the testing chamber where the locations of the subjects were tracked and recorded using Noldus EthoVision XT video tracking software. Two zones (left and right) on either end of the box (30 × 30 cm) as well as a neutral zone in the centre of the box (10 cm) were denoted as part of the arena settings. Mice were introduced in the neutral zone of the empty arena and allowed to explore freely for 3 min. The tracking software monitored which of the two zones each individual mouse preferred. After 3 min, the experimenter introduced two objects (empty methanol bottle or cryostat liquid bottle (sealed)) and placed them in the middle of the left and right zones. For each mouse, one of the objects was the same as the one experienced during training (target object in target zone) and was placed in the least preferred zone. The other object was novel (novel side) and placed in the preferred side. During minutes 6 to 9, objects were absent from the arena. During minutes 9 to 12, the objects were reintroduced in the same positions as minutes 3 to 6.

Cell counting. The number of mCherry or c-Fos immunoreactive neurons in the dentate gyrus and downstream areas were counted to measure the number of active cells during defined behavioural tasks in 3–5 coronal slices (spaced 160 μm from each other) per mouse. Only slices that showed accurate bilateral injections in the dentate gyrus were selected for counting. Fluorescence images were acquired using a microscope with a ×20/0.50 NA objective. All animals were sacrificed 90 min post-assay or optical stimulation for immunohistochemical analyses. The number of c-Fos-positive cells in a set region of interest (0.5 mm^2 per brain area analysed) were quantified with ImageJ and averaged within each animal. Background autofluorescence was accounted for by applying an equal cut-off threshold to all images by an experimenter blind to experimental conditions. To calculate the percentage of BLA, mPFC, or NAcc cells expressing ArchT–eGFP in Fig. 3c, we counted the number of GFP-positive cells and divided by the total number of DAPI-positive cells in each region. Statistical chance was calculated by multiplying the observed percentage of ArchT–GFP-single-positive cells by the observed percentage of c-Fos-single-positive cells; overlaps over chance were calculated as observed overlap divided by chance overlap: $\frac{\left(\frac{\text{GFP}^+ \times \text{c-Fos}^+}{\text{DAPI}}\right)}{\text{chance overlap}}$.

A one-way ANOVA followed by Tukey's multiple comparisons or one-sample *t*-tests were used to analyse data and later graphed using Microsoft Excel with the Statplus plug-in or Prism.

Neurogenesis. After all the behaviour tests, on the 15th day since the first day of light stimulation, the mice were overdosed with Avertin and perfused transcardially with cold phosphate buffer saline (PBS), followed by 4% paraformaldehyde (PFA) in PBS. Brains were extracted from the skulls and kept in 4% PFA at 4 °C overnight. Coronal slices 50-μm thick were taken using a vibratome and collected in cold PBS. For immunostaining, each slice was placed in PBST (PBS + 0.2% Triton X-100) with 5% normal goat serum for 1 h and then incubated with primary antibody at 4 °C for 24 h (1:250 mouse anti-PSA-NCAM, Millipore; 1:500 doublecortin, AB2253, Millipore). Slices then underwent three wash steps for 10 min each in PBST, followed by a 1 h incubation period with secondary antibody (PSA-NCAM: 1:250 AlexaFluor488 anti-mouse, Invitrogen; Doublecortin: 1:300 A21435, Invitrogen). Slices were then incubated for 15 min with 4′,6-diamidino-2-phenylindole (DAPI; 1:10,000) and underwent three more wash steps of 10 min each in PBST, followed by mounting and coverslipping on microscope slides. Images were taken using a Zeiss Axio Imager2 microscope. PSA-NCAM$^+$ or doublecortin$^+$ cells in the dentate gyrus granule cell layer were counted and normalized to the area of the granule cell layer for each brain slice using ImageJ by a researcher blind to the identities of each animal. After all the data were collected, the identities of each animal were revealed and the data were assigned back into each group for statistical analysis.

***In vivo* electrophysiology.** As described above, three mice were first bilaterally injected with an AAV_9-TRE-ChR2-mCherry virus into the dentate gyrus followed by lowering a bilateral optic fibre implant into position and cementing it to the skull. Following 10 days for recovery and viral expression, in a separate surgery, mice were chronically implanted with a hyperdrive that housed six independently moveable tetrodes targeting the BLA. To accommodate the optic fibre implant cemented on the skull, the AP coordinate for the hyperdrive was adjusted slightly (centred at AP = −0.85 mm) and implanted at a ∼15° angle. The electrical signal recorded from the tips of the tetrodes was referenced to a common skull screw over the cerebellum and differentially filtered for single unit activity (200 Hz to 8 kHz) and local field potentials (1–200 Hz). The amplified signal from each wire is digitized at 40 kHz and monitored with an Omniplex sytem (Plexon). Action potentials from single neurons were isolated off-line using time–amplitude window discrimination through Offline Sorter (Plexon). Putative single units were isolated by visualizing combinations of waveform features (square root of the power, peak–valley, valley, peak, principal components, and time-stamps) extracted from wires composing a single tetrode. The average firing rate for isolated neurons was 2.25 Hz ± 4.14 Hz (mean ± s.d.; range 0.01–30.15 Hz). However, the firing rate distribution was highly rightward skewed (median: 0.81 Hz) and more than half of the neurons (62%; 66/106) had firing rates under 1 Hz. After the last recording session, small lesions were made near the tips of each tetrode by passing current (30 μA for ∼10 s) and mice were transcardially perfused and brains extracted for histology using standard procedures.

Recording and light stimulation protocol. Each mouse had two recording sessions that occurred on two different days separated by 72 h. Mice were first placed into a small recording chamber. In a single recording session, mice were first bilaterally stimulated in the dentate gyrus with blue light (450 nm; Doric Lenses) for 10 s over 15 such trials in total. As a control, the blue light was replaced with red light (640 nm; Doric Lenses) and the mice were given twelve 10-s trials under this condition. The power output for the blue and red lights emitted from the tips of each patch cord was adjusted to 15–18 mW as measured with a standard photometer (Thor Labs). The blue and red lasers were powered using a laser diode driver (Doric Lenses) triggered by transistor–transistor logic (TTL) pulses emitted from a digital I/O card, and these events were also time-stamped and recorded in the Omniplex system. The recording session lasted ∼20 min and each tetrode was lowered ∼0.25 mm after the first recording session.

Electrophysiological data analysis. Spiking activity was analysed using commercial (Neuroexplorer, NEX Technologies) and custom-made software in Matlab (R2014B). To visualize each neuron's trial-averaged activity for the blue and red light stimulation period, a peristimulus time histogram (PSTH) with 100-ms time bins was generated with activity time locked to the onset of the blue or red light, and then smoothed with a Gaussian kernel (θ = 127 ms). In order to confirm a response during blue or red light stimulation period, 99% confidence intervals were constructed for the trial-averaged activity using a baseline 2.5 s period of spiking activity before the onset of each light under the assumption of Poisson spiking statistics (for example, Neuroexplorer, NEX Technologies). A neuron was considered to have a response for a particular light stimulation condition if trial averaged activity exceeded the upper (excitatory) or lower (inhibitory) bound of the 99% confidence interval. We considered neurons activated from dentate gyrus stimulation when a neural response was confirmed for the blue light condition but not the red light condition. For each neuron identified as such, we *z*-scored neural activity depicted in the blue and red light PSTH, then identified the maximum trial-averaged *z*-score value from the 2.5 s baseline (Pre) and during blue or red light stimulation (Post). The Pre and Post maximum *z*-score values for the blue and red light stimulation period was compared using paired *t*-tests (Fig. 2p).

31. Reijmers, L. G., Perkins, B. L., Matsuo, N. & Mayford, M. Localization of a stable neural correlate of associative memory. *Science* **317,** 1230–1233 (2007).
32. Redondo, R. L. *et al.* Bidirectional switch of the valence associated with a hippocampal contextual memory engram. *Nature* **513,** 426–430 (2014).
33. Ramirez, S. *et al.* Creating a false memory in the hippocampus. *Science* **341,** 387–391 (2013).
34. Liu, X. *et al.* Optogenetic stimulation of a hippocampal engram activates fear memory recall. *Nature* **484,** 381–385 (2012).
35. Han, X. *et al.* A high-light sensitivity optical neural silencer: development and application to optogenetic control of non-human primate cortex. *Front. Syst. Neurosci.* **5,** 18 (2011).
36. Huff, M. L., Miller, R. L., Deisseroth, K., Moorman, D. E. & LaLumiere, R. T. Posttraining optogenetic manipulations of basolateral amygdala activity modulate consolidation of inhibitory avoidance memory in rats. *Proc. Natl Acad. Sci. USA* **110,** 3597–3602 (2013).
37. Snyder, J. S., Soumier, A., Brewer, M., Pickel, J. & Cameron, H. A. Adult hippocampal neurogenesis buffers stress responses and depressive behaviour. *Nature* **476,** 458–461 (2011).

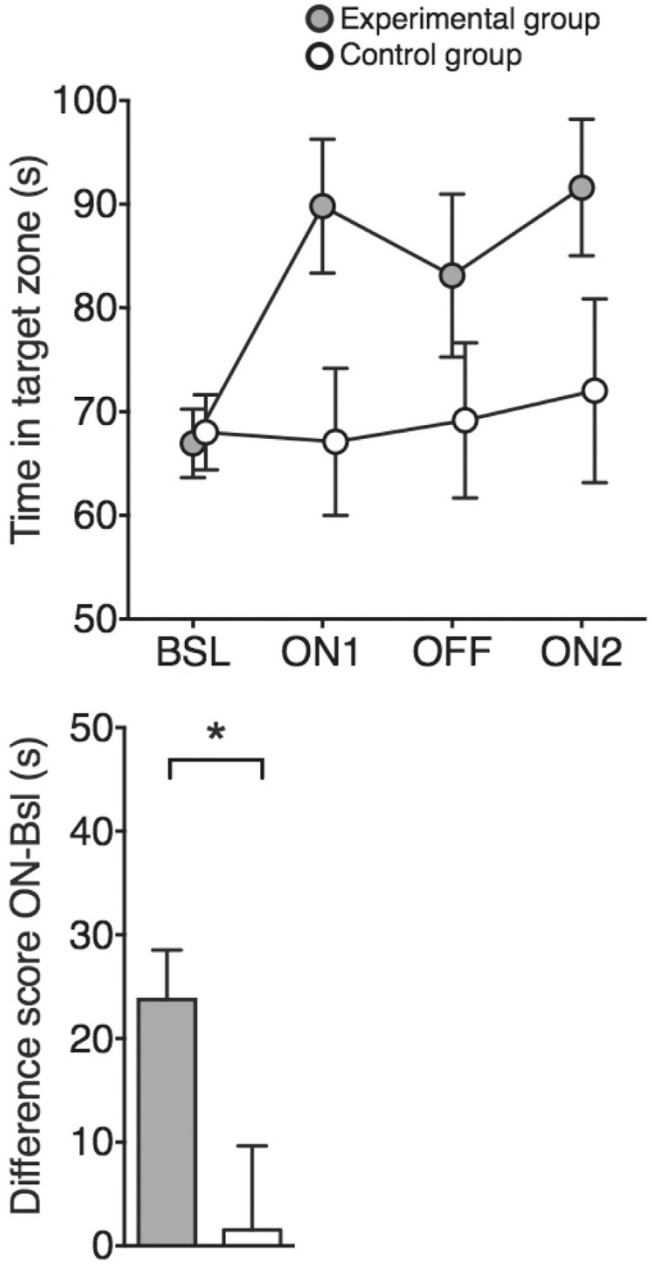

Extended Data Figure 1 | Male mice spend more time around an object associated with females. Top, Time spent in the target zone where the object associated with females is introduced in the ON phases. Female-object paired mice (experimental group) spend more time in the target zone during the ON phases than the neutral-object paired mice (control group; two-way ANOVA with multiple comparisons, ON1 $t_{88} = 2.41$; $P < 0.05$, ON2 $t_{88} = 2.08$; $P < 0.05$). Bottom, Difference score (average of ON phases − baseline (Bsl)) also shows the increased preference for the target zone in the female-object group compared to neutral-object group ($t_{22} = 2.37$; $^*P < 0.05$). $n = 12$ per group. See the Methods section for detailed methods.

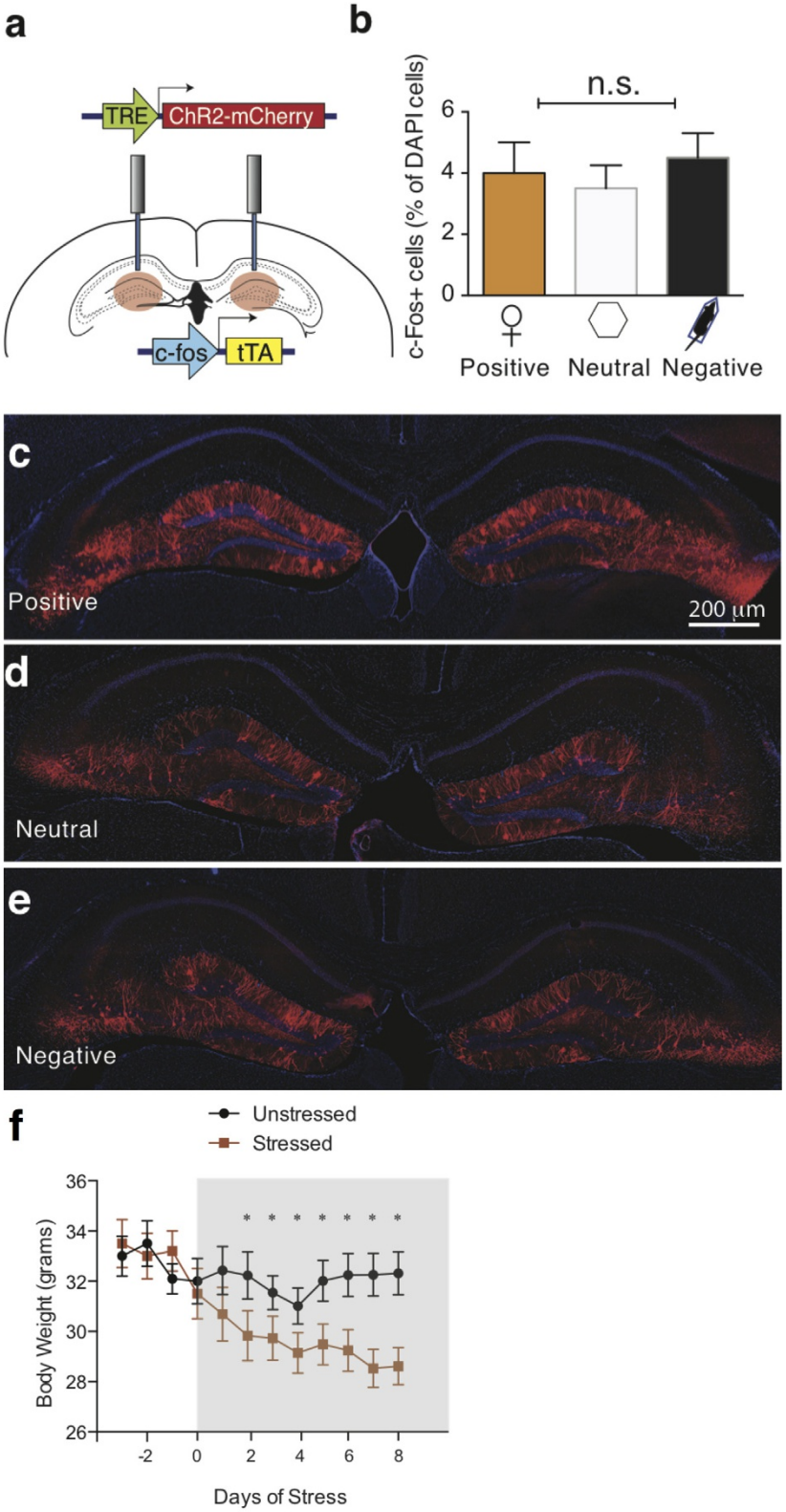

Extended Data Figure 2 | Positive, neutral, or negative experiences label a similar proportion of dentate gyrus cells with ChR2; stress prevents weight gain over 10 days. **a**, The c-Fos mice were bilaterally injected with AAV_9-TRE-ChR2-mCherry and implanted with optical fibres targeting the dentate gyrus. **b–e**, Histological quantifications reveal that, while off Dox, a similar proportion of dentate gyrus cells are labelled by ChR2–mCherry in response to a positive (**c**), neutral (**d**), or negative (**e**) experience. All animals were sacrificed a day after completing the CIS protocol. One-way ANOVA followed by Bonferroni post hoc test, $P > 0.05$, n.s., not significant. **f**, Animals were chronically immobilized for 10 days, during which they lost a significant amount of weight compared to an unstressed group (one-way ANOVA followed by Bonferroni post hoc test, $^*P < 0.05$, $n = 9$ per group). Data are means ± s.e.m.

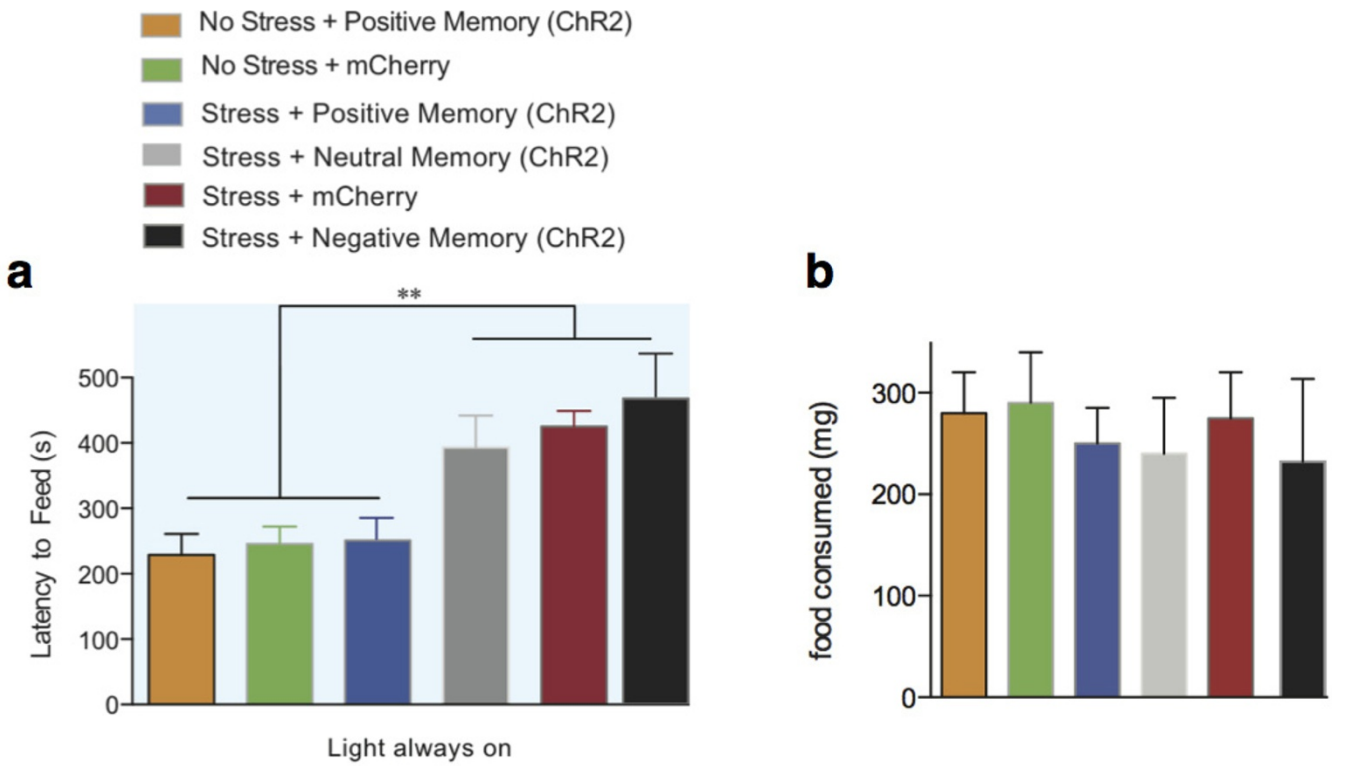

Extended Data Figure 3 | Reactivation of a positive memory decreases latency to feed in a novelty suppressed feeding paradigm. a, All groups were food deprived for 24 h and then underwent a novelty-suppressed feeding protocol. While chronic immobilization increased the latency to feed, light-reactivation of a positive memory significantly decreased the latency to feed at levels that matched the unstressed groups. **b**, Upon completion of the novelty suppressed feeding test, all groups were returned to their home cage and food intake was measured after 5 min (one-way ANOVA followed by Bonferroni post hoc test, $^{**}P < 0.01$, $n = 16$ per group). Data are means ± s.e.m.

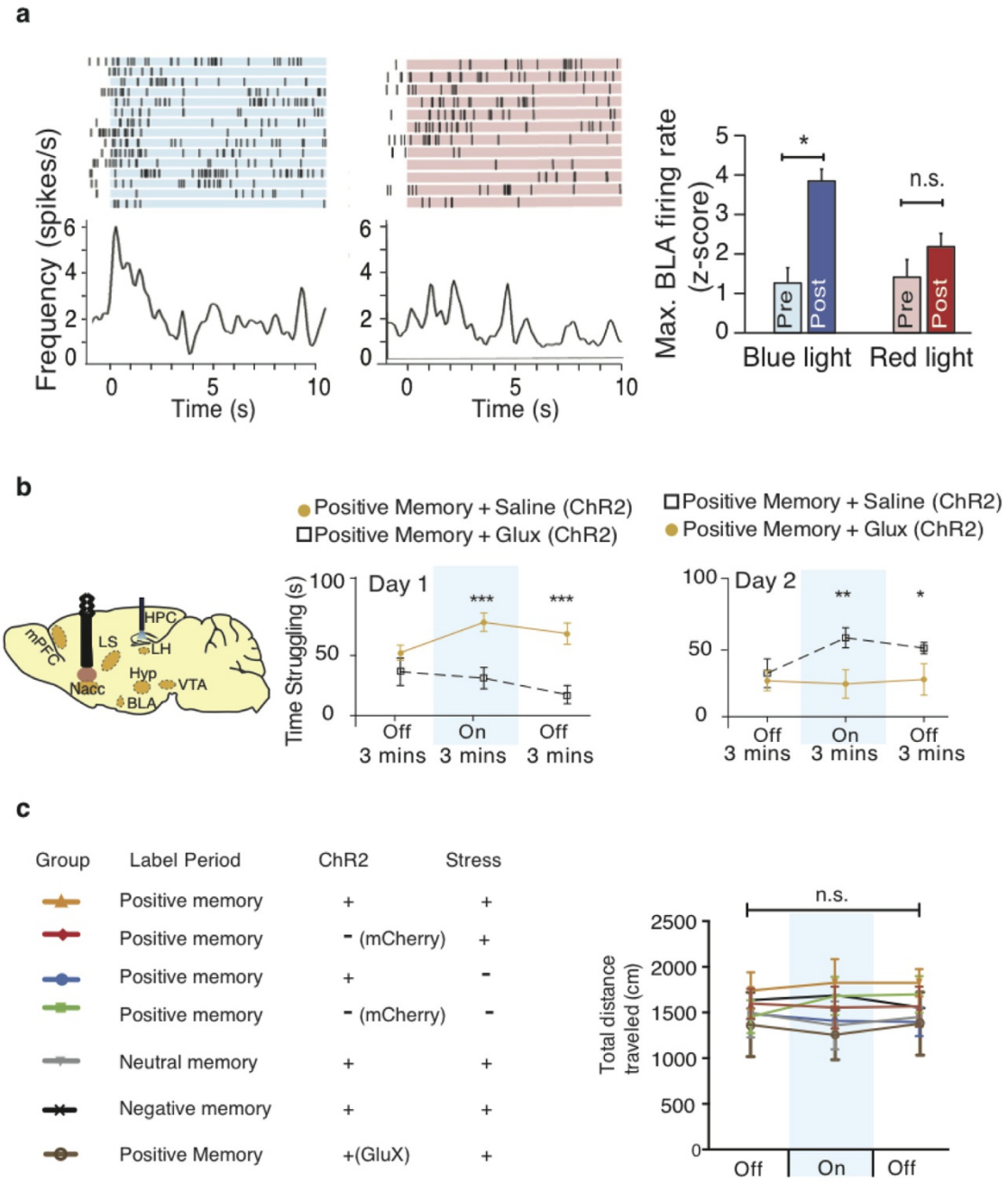

Extended Data Figure 4 | Activation of a positive memory elicits BLA spiking activity, requires NAcc glutamatergic activity in the tail suspension test, but does not alter locomotor activity in the open field test. **a**, Raster plots and peri-stimulus time histograms (PSTH) illustrating a transient excitatory response from a single BLA neuron out of the nine neurons responsive to dentate gyrus positive memory activation during 10 s of blue light stimulation, but not in response to 10 s of red light as a control. Blue bar plots on the right illustrate maximum BLA neural firing rate before (Pre) and after (Post) blue light stimulation in the dentate gyrus (paired *t*-test, $t_7 = 6.91$, $^*P = 0.023$). Red bar plots show the maximum neural activity for the same neurons after red light stimulation in the dentate gyrus that serves as a control (paired *t*-test, $t_7 = 1.62$, $P = 0.15$). **b**, Brain diagram illustrating target areas manipulated. Within-subjects experiments revealed that glutamatergic antagonists (Glux), but not saline, in the accumbens shell blocked the light-induced effects of a positive memory in stressed subjects. For behavioural data, a two-way ANOVA with repeated measures followed by a Bonferroni post hoc test revealed a group-by-light epoch interaction on day 1 ($F_{1,90} = 28.39$, $P < 0.001$; $n = 16$ per group) and day 2 of testing ($F_{1,90} = 8.28$, $P < 0.01$). Data are means ± s.e.m. **c**, All groups failed to show significant changes in locomotor activity within a session of open field exploration during either light off or light on epochs, though any trends towards decreases in locomotion are consistent with stress-induced behavioural impairments. $^*P < 0.05$, $^{**}P < 0.01$, $^{***}P < 0.001$.

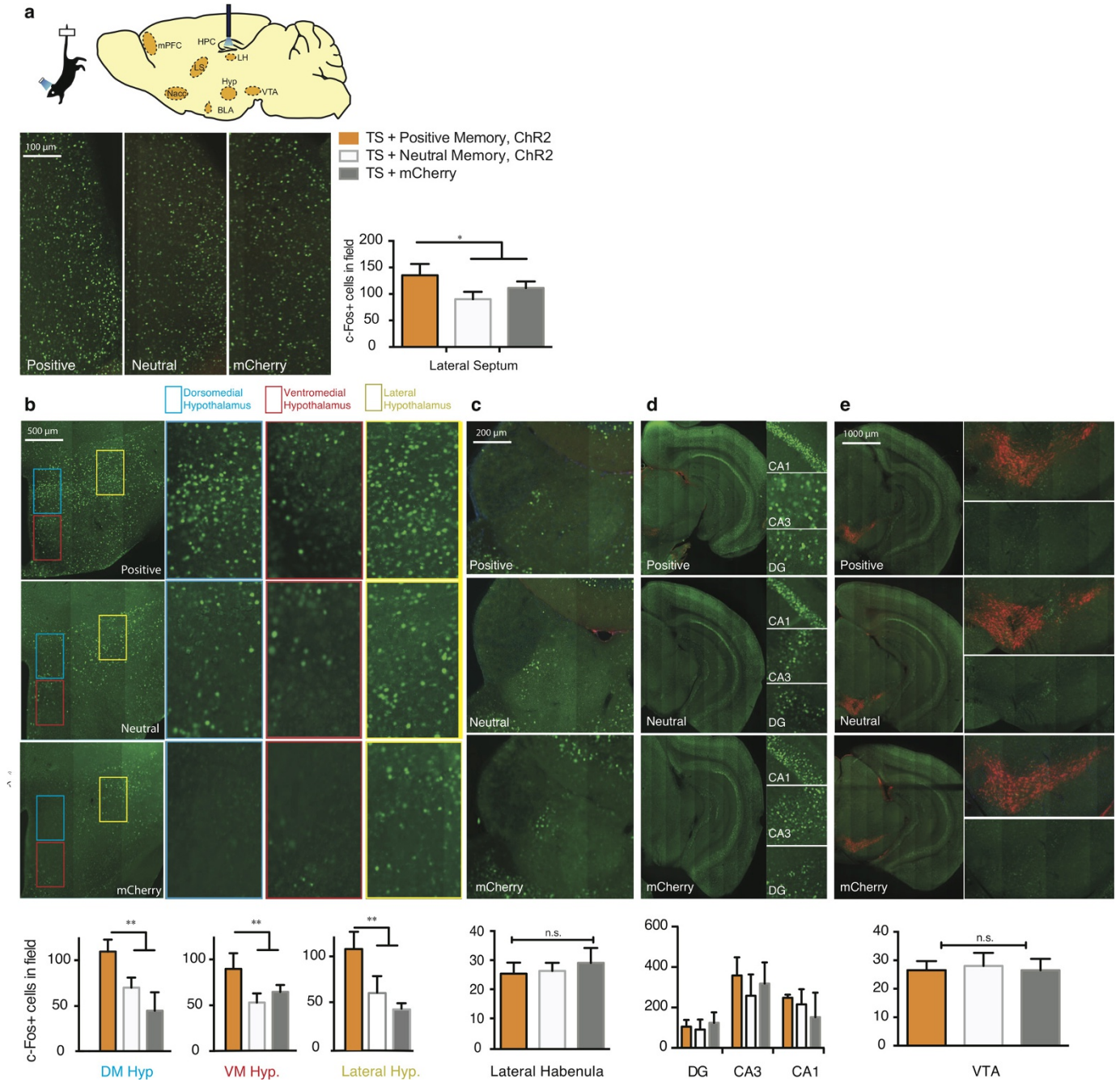

Extended Data Figure 5 | Activating a positive memory in the dentate gyrus produces an increase in c-Fos expression in the lateral septum and hypothalamus, but not the lateral habenula, ventral hippocampus, or VTA. **a**, Diagram of regions analysed. **b**, **c**, c-Fos expression significantly increased in the lateral septum (**b**) and subregions of the hypothalamus including the dorsomedial (DM), ventromedial (VM), and lateral hypothalamus (**c**) in the positive memory group but not in a group in which a neutral memory was stimulated or in a group expressing mCherry alone. **c**–**e**, c-Fos expression did not significantly increase in the lateral habenula (**c**), various ventral hippocampus subregions (**d**), or VTA, identified by tyrosine hydroxylase staining (red) stainings in the images expanded on the right (**e**) (one-way ANOVA followed by Bonferroni post hoc test $^{*}P < 0.05$, $^{**}P < 0.01$, $n = 5$ animals per group, 3–5 slices per animal). TS, tail suspension. Data are means ± s.e.m.

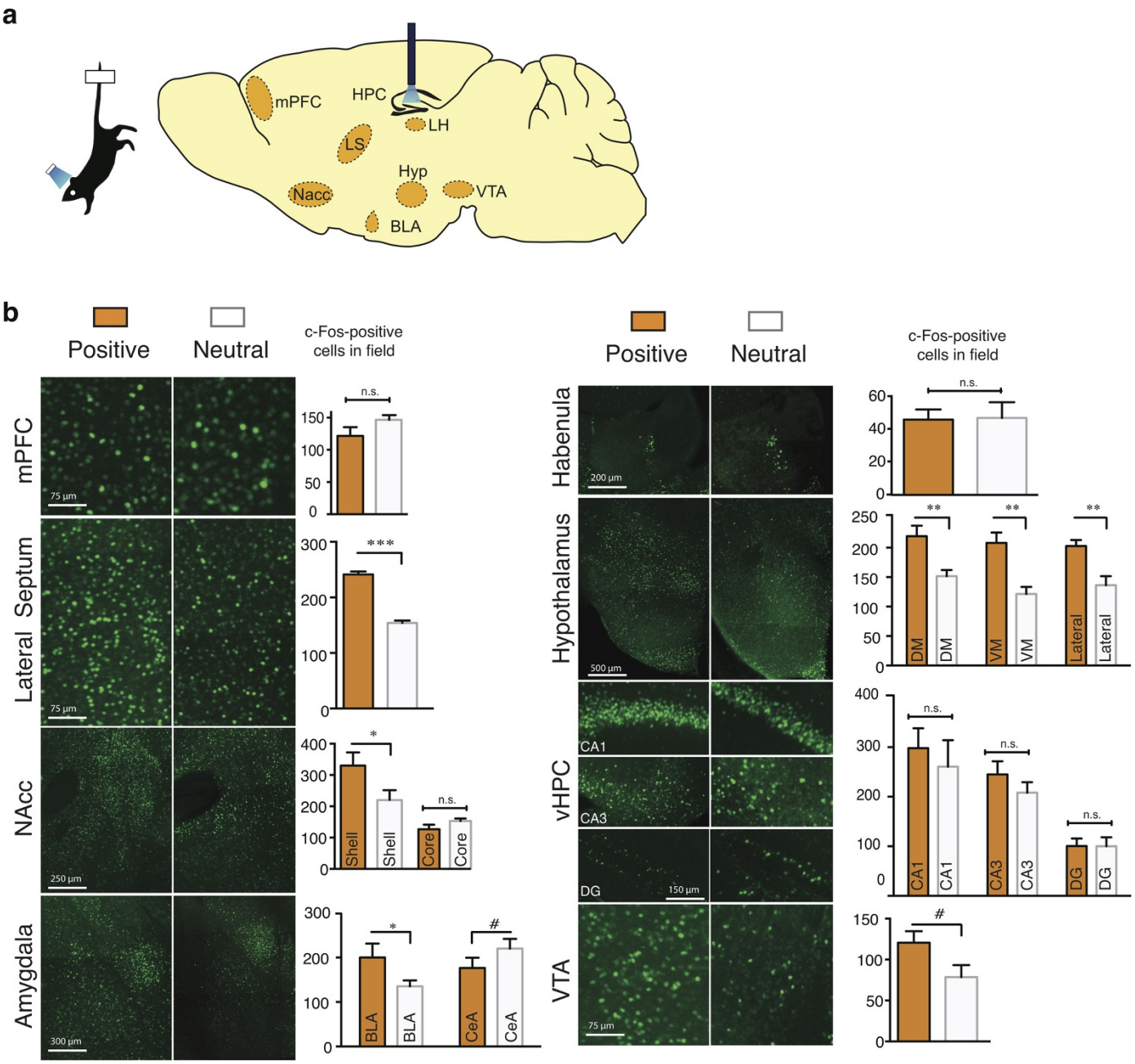

Extended Data Figure 6 | Activating a positive memory through the dentate gyrus of unstressed animals increases c-Fos expression in various downstream regions. **a**, Diagram of regions analysed. **b**, In the positive compared to the neutral memory group, c-Fos expression is significantly increased in the lateral septum, NAcc shell, BLA, dorsomedial, ventromedial and lateral hypothalamus, but not in the mPFC, NAcc core, habenula, or ventral hippocampus. Trends were observed in the central amygdala (CeA) and VTA. Each brain region was analysed using an unpaired Student's *t* test, $n = 5$ animals per group, 3–5 slices per animal; $\#P = 0.17$ for central amygdala and $P = 0.09$ for VTA; $*P < 0.05$, $**P < 0.01$, $***P < 0.001$, n.s., not significant. Data are means ± s.e.m.

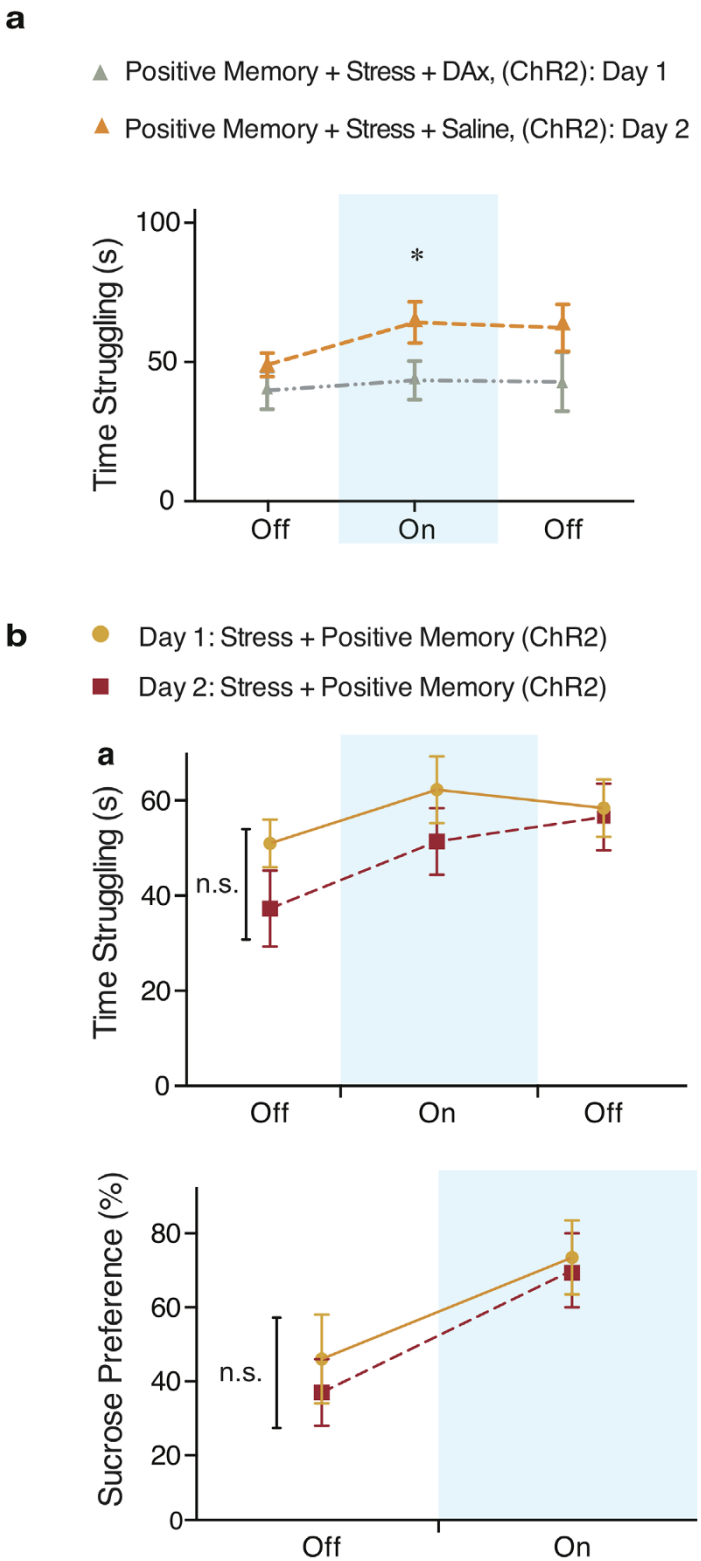

Extended Data Figure 7 | Dopamine receptor antagonists block the light-induced effects of positive memory activation; a single session of activating a positive memory in the dentate gyrus does not produce long-lasting antidepressant-like effects. **a**, Administration of a cocktail of dopamine receptor antagonists (DAx) prevented the light-induced increases in struggling during the tail suspension test. When animals were tested again on day 2 and infused with saline, the behavioural effects of optically reactivating a positive memory were observed (two-way ANOVA with repeated measures followed by Bonferroni post hoc test, $^{*}P < 0.05$, $n = 9$ per group). **b**, Animals in which a positive memory was optically activated during the tail suspension test or sucrose preference test showed acute increases in time struggling or preference for sucrose; this change in behaviour did not persist when tested again on day 2 (within subjects ANOVA followed by Bonferroni post hoc test), $n = 9$. n.s., not significant. Data are means ± s.e.m.

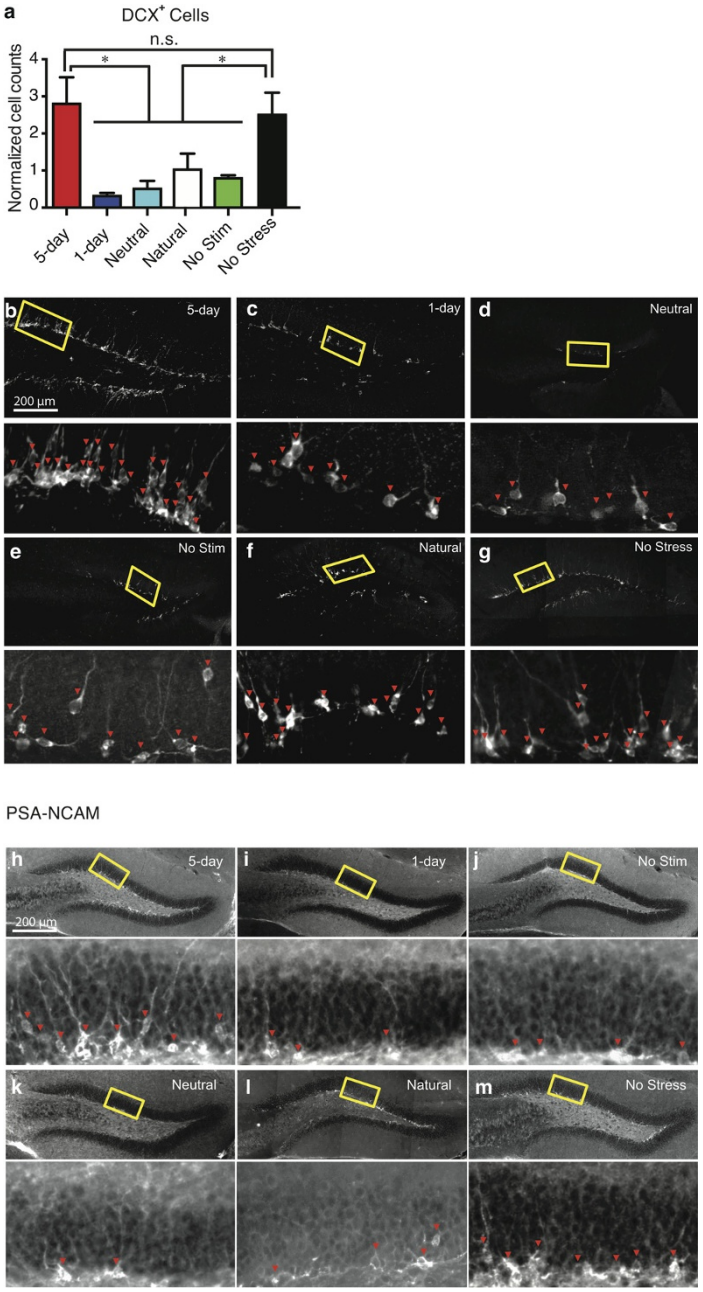

Extended Data Figure 8 | Chronic activation of a positive memory prevents stress-induced decreases in neurogenesis. **a**, The 5-day positive memory stimulation group showed a significant increase of adult newborn cells in the dentate gyrus as measured by doublecortin (DCX)-positive cells (one-way ANOVA followed by Bonferroni post hoc test, $F_{5,72} = 7.634$, $P < 0.01$) relative to control groups. **b**–**g**, Representative images of DCX-positive cells in the dentate gyrus for the 5-day (**b**), 1-day (**c**), neutral (**d**), no stimulation (**e**), natural (**f**), and no stress (**g**) groups. **h**–**m**, Representative PSA-NCAM images corresponding to data appearing in Fig. 4d. $n = 5$ slices per animal, 13 animals per group for data appearing in **a**. *$P < 0.05$, n.s., not significant. Data are means ± s.e.m.

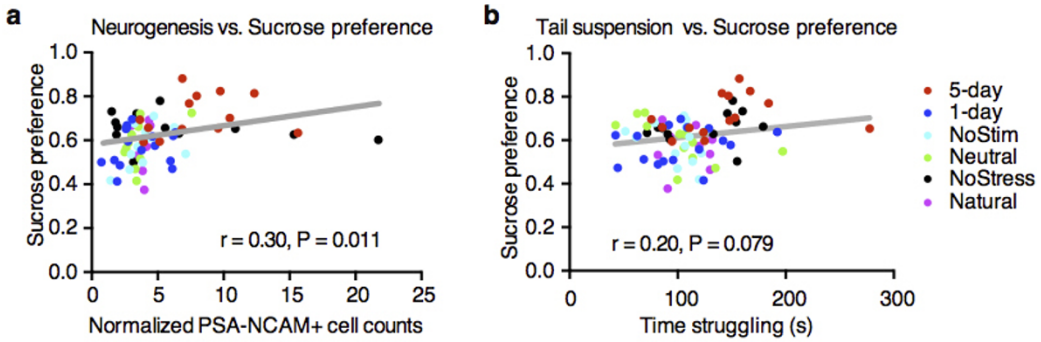

Extended Data Figure 9 | Behavioural and neuronal correlations. **a**, Performance levels in the SPT and the number of adult-born neurons as measured by PSA-NCAM are positively correlated on an animal-by-animal basis. **b**, Performance levels between the TST and SPT show strong positive correlation trends on an animal-by-animal basis. $n = 14$ per TST behavioural group, $n = 15$ per SPT behavioural group.